Phytochemistry Letters 10 (2014) 132–139

Contents lists available at ScienceDirect

Phytochemistry Letters

journal homepage: www.elsevier.com/locate/phytol

Phenylpropanoid glycosides of *Mimulus guttatus* (yellow monkeyflower)

Ken Keefover-Ring [a,b,*], Liza M. Holeski [a,1], M. Deane Bowers [c], Allen D. Clauss [d,2], Richard L. Lindroth [a]

[a] Department of Entomology, University of Wisconsin – Madison, 1630 Linden Drive, Madison, WI 53706, USA
[b] Umeå Plant Science Centre, Department of Plant Physiology, Umeå University, 90187 Umeå, Sweden
[c] Department of Ecology and Evolutionary Biology, University of Colorado, N122 Ramaley, Boulder, CO 80309, USA
[d] Department of Chemistry, University of Wisconsin – Madison, 1101 University Avenue, Madison, WI 53706, USA

ARTICLE INFO

Article history:
Received 8 July 2014
Received in revised form 21 August 2014
Accepted 24 August 2014
Available online 4 September 2014

Keywords:
Mimulus guttatus
Phenylpropanoid glycosides
Mimuloside
Conandroside
Verbascoside
Calceolarioside

ABSTRACT

Yellow monkeyflower [*Mimulus guttatus* DC., (Phyrmaceae)] has long been a model plant species for studies in genetics, evolution, and ecology, including plant–animal interactions. Nonetheless, exceedingly little is known about its secondary chemistry. We have discovered that the foliage of yellow monkeyflower contains a diverse suite of phenylpropanoid glycosides (PPGs); a class of compounds with many known biological activities. Using ^{1}H and ^{13}C NMR and UV and MS chromatography techniques, we positively identified five PPGs from the leaves of yellow monkeyflower. Four of these compounds occur in other species and one is previously undescribed. We also present UV and high-resolution tandem MS data that putatively identify 11 additional foliar compounds as PPGs. This initial discovery and elucidation of yellow monkeyflower's secondary chemistry will be important for continued study of the genetics and ecology of this model species.

1. Introduction

Yellow monkeyflower [*Mimulus guttatus* DC. (Phyrmaceae)] has emerged as a model system for integrated studies of genetics, evolution, and ecology, including plant-insect interactions (Eubanks et al., 2005; Fenster and Ritland, 1994; Hall and Willis, 2005; Holeski et al., 2013; Mojica et al., 2012; Wu et al., 2008). Yellow monkeyflower protects itself from herbivores with physical defenses in the form of trichomes, which have been well studied (Holeski, 2007; Holeski et al., 2010; Scoville et al., 2011). Similarly, the foliar surface secondary compounds of plants in this genus have been explored in several studies. For instance, Bohm (1992) described flavonoids from the leaf exudate of *Mimulus lewisii* and both Lincoln and Walla (1986) and Hare (2002a, 2002b) found that the surface leaf resins of *Mimulus aurantiacus* contain a variety of geranylflavanones and an α-pyrone. Additional work with ground leaf extracts identified compounds similar to these leaf resins in other *Mimulus* species (Piovano et al., 2009; Salem et al., 2011). In contrast, other than a report of the compound responsible for the yellow flower color (Nitsche et al., 1969), very little is known about the internal secondary metabolism of yellow monkeyflower (Holeski et al., 2013) or any other species in the genus. Absent a thorough understanding of the signature secondary metabolites of *M. guttatus*, its utility as a model species for studies of ecological and evolutionary interactions is limited.

We have discovered that yellow monkeyflower synthesizes a suite of mono- and disaccharide phenylpropanoid glycosides (PPGs; aka, phenylethanoid glycosides, Jimenez and Riguera, 1994; or caffeic acid esters, Mølgaard and Ravn, 1988) in its foliage. PPGs originate from the shikimic acid-phenylpropanoid pathway and include simple monosaccharides, consisting of hydroxycinnamic acid and hydroxyphenylethyl moieties bonded to a central β-glucopyranose by ester and glycosidic linkages, respectively, and more complex di- and trisaccharides with one or two additional sugars linked to the core glucose (Jimenez and Riguera, 1994; Mølgaard and Ravn, 1988). Members of this compound class have shown a wide range of biological activity, including inhibition of plant pathogenic bacteria and fungi (Ravn et al., 1989), antioxidant

* Corresponding author at: Department of Entomology, University of Wisconsin – Madison, 1630 Linden Drive, Madison, WI 53706, USA. Tel.: +1 6085092265.
E-mail address: keefover@entomology.wisc.edu (K. Keefover-Ring).
[1] Current address: Department of Biological Sciences, University of Northern Arizona, 617 S. Beaver Street, Flagstaff, AZ 86011, USA.
[2] Current address: Xolve, Inc., 1600 Aspen Commons, Suite 101, Middleton, WI 53562, USA.

http://dx.doi.org/10.1016/j.phytol.2014.08.016
1874-3900/

activity (Cardinali et al., 2012; Jimenez and Riguera, 1994; Owen et al., 2003), tumor cell suppression (Chen et al., 2002; Jimenez and Riguera, 1994), feeding stimulation of specialist herbivores (Holeski et al., 2013), and deterrence of generalist insects (Cooper et al., 1980; Mølgaard, 1986). In addition, recent work has shown that these compounds can vary considerably among natural populations and between annual and perennial ecotypes of yellow monkeyflower (Holeski et al., 2013).

We used various liquid chromatography techniques to isolate and purify these compounds, and then identified them with a combination of ^{1}H and ^{13}C NMR and high-resolution tandem mass spectrometry. The characterization of this group of secondary metabolites in yellow monkeyflower represents an important advance in the continued study of plant-insect interactions with this important model species.

2. Results and discussion

Almost all plant species with available genomes and prominent secondary metabolism have well-characterized chemistry. For instance, *Arabidopsis thaliana* contains glucosinolates (Shroff et al., 2008), black cottonwood (*Populus trichocarpa*) produces phenolic glycosides (Boeckler et al., 2011), and Norway spruce (*Picea abies*) synthesizes terpenoids (Schmidt et al., 2010). Despite having a sequenced genome (http://www.mimulusevolution.org/), however, the internal foliar secondary chemistry of yellow monkeyflower has remained unknown.

The presence of a diverse suite of PPGs in the foliage of *M. guttatus* (Phrymaceae) is not surprising, given its relatedness to the Scrophulariaceae (Beardsley and Olmstead, 2002). The Scrophulariaceae contains a rich diversity of PPGs and is one of the few plant families with mono-, di-, and trisaccharide PPGs (Mølgaard and Ravn, 1988). In addition, while PPGs occur in many other plant families, most notably in the Oleaceae and Orobanchaceae, Jimenez and Riguera (1994) list the Scrophulariaceae as having the greatest number of species with this class of secondary metabolites. With this in mind, we investigated yellow monkeyflower foliage for the presence of PPGs with the goal of incorporating knowledge of secondary metabolism into future studies of *Mimulus* evolution, genetics, and ecology.

Using NMR and liquid chromatography with UV and MS detection, we positively identified five PPGs from the leaves of yellow monkeyflower. Four of these compounds occur in various other species and one appears to be previously undescribed. We also present UV and high-resolution MS/MS data that putatively identify 11 additional compounds as PPGs.

2.1. NMR results

The ^{1}H and ^{13}C NMR chemical shifts of four of the compounds isolated from yellow monkeyflower closely match those of previously described phenylpropanoid glycosides (Fig. 1, Table 1, Suppl. Table 1, and Suppl. Figs. S1 and S2). The 1D-NMR spectra of compounds **1** and **2** correspond to those reported by several researchers for calceolarioside A and B, respectively (Chen et al., 2009; Damtoft and Jensen, 1994; Iossifova et al., 1999; Nicoletti et al., 1986; Shimomura et al., 1987). Both calceolarioside A and B are monosaccharide PPGs, which Nicoletti et al. (1986) initially isolated from *Calceolaria hypericina* (Calceolariaceae). These substances are positional isomers with the caffeoyl moiety at either C-4′ (calceolarioside A) or C-6′ (calceolarioside B) of glucose; apparent from the ^{1}H and ^{13}C chemical shift reversal we observed at those positions (Suppl. Table 1). HMBC correlations further confirmed the side group positions on compounds **1** and **2** (Suppl. Table 1). For instance, in calceolarioside A (**1**), HMBC correlations between H-4′ and C=O and the reciprocal correlations of H-1′ to C-8 and of the C-8 protons to C-1′ demonstrated the location of the caffeoyl and hydroxyphenylethyl groups, respectively. PPGs **3**–**5** displayed these same HMBC correlations, confirming that their hydroxycinnamic acid and hydroxyphenylethyl moieties have the same positions as those in calceolarioside A (**1**). Calceolarioside B (**2**), however, showed a correlation between both H-6′ protons and C=O, due to the alternative attachment of the caffeoyl group. Calceolarioside A corresponds to PPG 4 in our earlier work on variation of PPGs in natural populations of yellow monkeyflower (Holeski et al., 2013).

The 1D-NMR spectra of compound **3** matches that of conandroside (Jensen, 1996; Nonaka and Nishioka, 1977), a PPG originally isolated from *Conandron ramoidioides* (Nonaka and Nishioka, 1977). Unlike many other disaccharide PPGs, which have rhamnose as their side sugar, conandroside has a xylose bonded to C-3′ of the glucosyl moiety (Jimenez and Riguera, 1994; Mølgaard and Ravn, 1988). HMBC correlations of H-3′ to C-1″ and H-1″ to C-3′ further verified the specific connection of these two sugars (Suppl. Table 1).

NMR data identified compound **4** as verbascoside (Damtoft and Jensen, 1994; Nishimura et al., 1991; Owen et al., 2003), also known in much of the literature as acetoside, or less commonly kusaginin (Jimenez and Riguera, 1994; references therein). While overall very similar to conandroside (**3**), the ^{1}H NMR spectra of verbascoside (**4**) contained a doublet at δ_H 1.08 ppm, due to the three protons on the C-6″ methyl of the rhamnose side-sugar (Fig. 1). As with conandroside, HMBC data for verbascoside showed the same placement of this secondary sugar on the glucosyl moiety (Suppl. Table 1).

Compound **5** appears to be a new PPG (Søren Jensen, personal communication), which we have named mimuloside. Due to the presence of xylose as the secondary sugar, both the ^{1}H and ^{13}C NMR shifts of mimuloside closely match those of conandroside (**3**), except for additional distinctive shifts at δ_H 3.89 ppm and δ_C 56.44 ppm arising from the methoxy on the feruloyl moiety (Table 1, Suppl. Table 1; Chin et al., 2010; Froelich et al., 2008; Li et al., 2008). Furthermore, as with compounds **1**–**4**, the coupling constants of the α and β protons indicate a *trans*-configuration of the feruloyl group double bond (Nishimura et al., 1991). Thus, mimuloside is conandroside with ferulic instead of caffeic as its hydroxycinnamic acid.

The two-dimensional NMR results further confirmed the structure of mimuloside (**5**). HMBC correlations showed the same placement of both the hydroxycinnamic acid and hydroxyphenylethyl groups, as seen in **1**, **3**, and **4** (Table 1, Suppl. Table 1). A final key HMBC relationship included a correlation of the methoxy protons (δ_H 3.89) with C-3‴ of the feruloyl aromatic ring (δ_C 149.4), confirming mimuloside's hydroxycinnamic acid as ferulic (Li et al., 2008) and not the possible isoferulic acid seen on other PPGs, such as eukovoside (Stricher et al., 1982). We previously referred to mimuloside as PPG 5 in Holeski et al. (2013).

2.2. UHPLC-UV-TOF/MS results

The UV spectra of all compounds tested with UHPLC-UV-TOF/MS had very similar profiles with UV maxima near 327 nm (Table 2, Appendix 2), mostly due to UV activity of the hydroxycinnamic acid moiety (Pati et al., 2006; Li et al., 2005). These analyses also showed that individual plant samples differed greatly in the number of PPGs present and that the retention time of an authentic verbascoside standard closely matched that of compound **4** (Fig. 2, Appendix 2). Furthermore, extracted ion chromatograms for *m*/*z* 477 and 609 from TOF/MS analyses showed that some individual plant samples contained numerous isomers with these molecular weights (Fig. 2, Table 2).

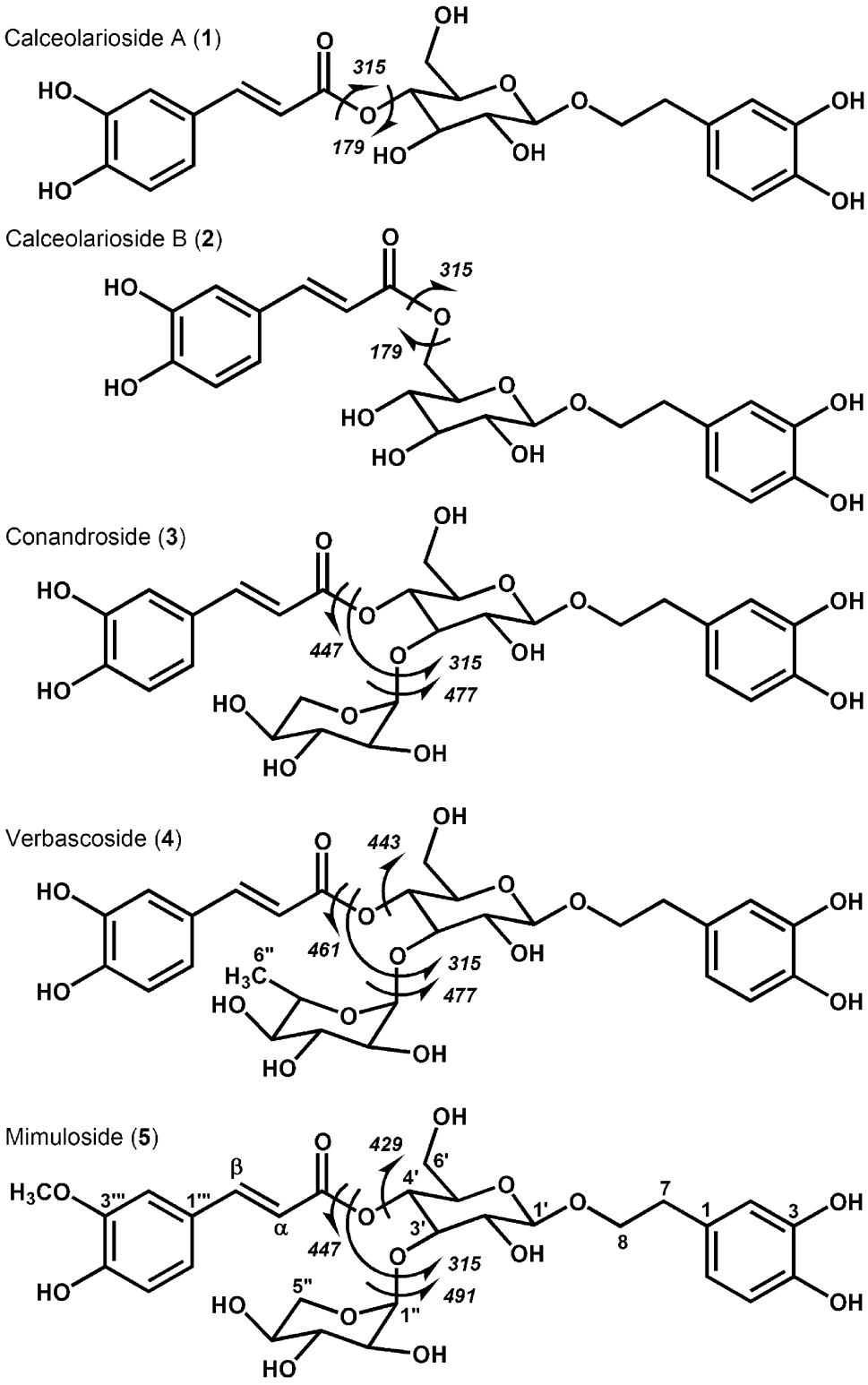

Fig. 1. Structures of five identified phenylpropanoid glycosides isolated from the foliage of *Mimulus guttatus*. Arrows and numbers in italics indicate the major MS/MS fragments. NMR designations used for all compounds appear on structures **4** and **5**.

2.3. High-resolution tandem MS results

The PPGs found in yellow monkeyflower foliage produced predictable MS/MS ion fragments due to the similar dissociation mechanisms (Fig. 1; Table 2; Appendix 1). First, the hydroxycinnamic acid moieties proved the most labile side groups. Compounds containing a caffeoyl group produced caffeic acid ion fragments of m/z 179 and those with a feruloyl moiety had ions of m/z 193, corresponding to ferulic acid. In addition, compounds with exact mass of 478 (precursor ion $[M-H]^-$ m/z 477) produced m/z 161 as a major fragment, which Ryan et al. (1999) assigned to a dehydrated caffeic acid ion. In all compounds, the loss of the hydroxycinnamic acid moieties resulted in the most abundant remaining fragments (i.e. m/z 447, 461, and 475), composed of the

Table 1
NMR spectroscopic data for mimuloside (**5**) in CD_3OD from the foliage of *Mimulus guttatus*. H-C designations confirmed with HSQC. Key HMBC correlations for structure elucidation in bold face. See Fig.1 for carbon designations.

C no.	δ_H	δ_C	COSY	HMBC
Hydroxyphenylethyl moiety				
1		131.4		
2	6.69 (*d*, 1.9)	117.1		36.6, 121.3, 144.7
3		146.1		
4		144.7		
5	6.67 (*d*, 8.0)	116.3	6	131.4, 146.1
6	6.56 (*dd*, 1.9, 8.0)	121.3	5	36.6, 117.1, 144.7
7	2.79 (*m*)	36.6	8	72.2, 117.1, 121.3, 131.4
8	3.72 (*m*); 4.04 (*m*)	72.2	7	36.6, **103.9**, 131.4
Glucosyl moiety				
1′	4.41 (*d*, 7.9)	103.9	2′	**72.2**, 76.0
2′	3.48 (*dd*, 7.9, 9.2)	74.9	1′, 3′	85.2, 103.9
3′	3.83 (*t*, 9.2)	85.2	2′, 4′	70.9, 74.9, **106.9**
4′	4.92 (*t*, 9.3)	70.9	3′, 5′	62.3, 76.0, 85.2, **168.4**
5′	3.54 (*m*)	76.0	4′, 6′	62.3, 70.9, 76.0, 85.2
6′	3.55 (*m*); 3.63 (*m*)	62.3	5′	70.9
Outer sugar moiety				
1″	4.44 (*d*, 7.6)	106.9	2″	67.3, **85.2**
2″	3.14 (*dd*, 7.6, 8.9)	75.7	1″, 3″	77.6, 106.9
3″	3.26 (*t*, 8.9)	77.6	2″, 4″	67.3, 71.0, 75.7
4″	3.34 (*m*)	71.0	3″, 5″	67.3, 77.6
5″	3.07 (*dd*, 11.3, 10.1); 3.62 (*m*)	67.3	4″	71.0, 77.6, 106.9
Hydroxycinnamic acid moiety				
1‴		127.7		
2‴	7.19 (*d*, 1.8)	111.7	6‴[a]	124.1, 147.1, 149.4, 150.7
3‴		149.4		
4‴		150.7		
5‴	6.81 (*d*, 8.2)	116.5	6‴	127.7, 149.4, 150.7
6‴	7.08 (*dd*, 1.8, 8.2)	124.1	2‴[a], 5‴	111.7, 147.1, 150.7
β	7.63 (*d*, 15.9)	147.1	α	111.7, 115.5, 124.1, 127.7, 168.4
α	6.36 (*d*, 15.9)	115.5	β	127.7, 168.4
C=O		168.4		
OCH_3	3.89 (*s*)	56.5		**149.4**

Multiplet and *J* (Hz) within parenthesis.
[a] Long range.

core glucose with both the hydroxyphenylethyl moetity and the secondary sugar still intact, also seen by Li et al. (2005). The size of these fragments varied due to an additional methoxy group on the hydroxyphenylethyl (possibly **15** and **16**) and/or the identity of the accessory sugar (xylose or rhamnose). In most of the compounds, these ions further fragmented to *m*/*z* 315, due to loss of the secondary sugar moiety in the disaccharide PPGs (Cardinali et al., 2012; Li et al., 2005), or simply from the initial loss of caffeic acid in the monosaccharides. These *m*/*z* 315 fragments also underwent dehydration, producing a *m*/*z* 297 ion (Cardinali et al., 2012), mostly apparent in the MS^3 spectra of the disaccharides. An ion of *m*/*z* 135 appeared in the MS^3 spectra of

Table 2
UHPLC-UV-MS/TOF and high-resolution MS/MS data for five identified and 11 putative phenylpropanoid glycosides from the foliage of *Mimulus guttatus*.

Compound	UV RT[a] (min)	UV λ_{max}[a] (nm)	Theoretical *m*/*z* $[M-H]^-$	Orbitrap LTQ[b]		Main MS/MS fragments[b]	
				m/*z* $[M-H]^-$	Formula	MS^2	MS^3
1	4.48	220, 328	477.1402	477.1408	$C_{23}H_{25}O_{11}$	161, **315**, 179, 297	135
2	4.65	218, 327	477.1402	477.1404	$C_{23}H_{25}O_{11}$	161, **315**, 281, 179	135
3	4.54	220, 328	609.1825	609.1825	$C_{28}H_{33}O_{15}$	**447**, 315, 477, 251	315, 135, 297
4	4.61	218, 331	623.1981	623.1974	$C_{29}H_{35}O_{15}$	**461**, 443, 477, 315	315, 135, 297
5	5.05	217, 326	623.1981	623.1978	$C_{29}H_{35}O_{15}$	**447**, 429, 491, 461	315, 135, 297
6	4.12	217, 326	477.1402	477.1406	$C_{23}H_{25}O_{11}$	161, **315**, 179, 203	135
7	4.28	217, 326	477.1402	477.1397	$C_{23}H_{25}O_{11}$	161, 315, 179, 203	np
8	4.77	216, 325	477.1402	477.1399	$C_{23}H_{25}O_{11}$	161, **315**, 179, 297	135
9	4.08	219, 329	609.1825	609.1824	$C_{28}H_{33}O_{15}$	**447**, 429, 477, 315	np
10	4.22	218, 327	609.1825	609.1818	$C_{28}H_{33}O_{15}$	**447**, 477, 429, 315	315, 135
11	4.32	218, 327	609.1825	609.1837	$C_{28}H_{33}O_{15}$	**447**, 477, 315, 301	315, 135, 297
12	4.71	218, 327	609.1825	609.1830	$C_{28}H_{33}O_{15}$	**447**, 315, 477, 297	315, 135, 297
13	4.91	218, 327	609.1825	609.1832	$C_{28}H_{33}O_{15}$	**447**, 315, 477, 251	315, 135, 297
14	5.08	218, 327	609.1825	609.1829	$C_{28}H_{33}O_{15}$	447, 315, 477	np
15	5.53	220, 325	637.2138	637.2146	$C_{30}H_{37}O_{15}$	461, 443, 505, 193	np
16	5.58	220, 329	651.2294	651.2297	$C_{31}H_{39}O_{15}$	475, 505, 457, 193	np

MS^2 precursor ion fragments used for MS^3 are in bold face. np, not performed.
[a] Data from UHPLC-UV-TOF/MS analyses.
[b] Data from high-resolution MS/MS analyses.

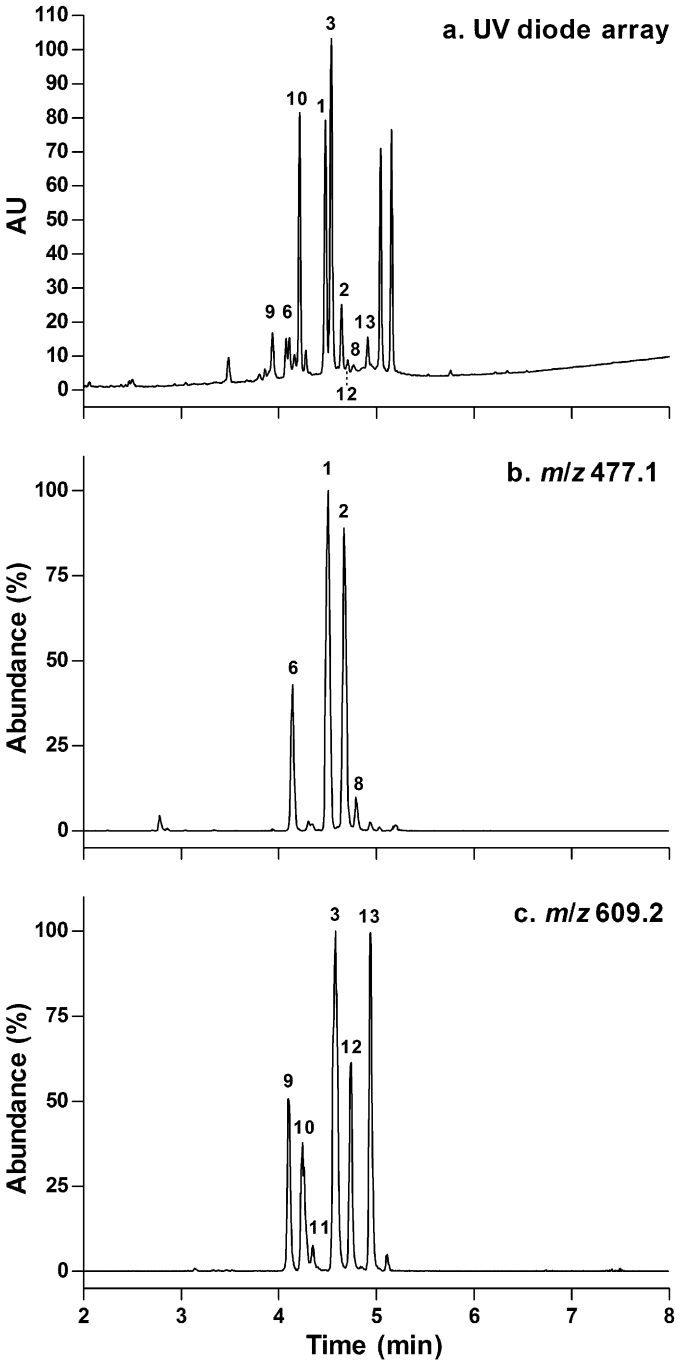

Fig. 2. Chromatograms of *Mimulus guttatus* individual 314 (population 12; see Table A1 in Appendix 2) from a single UHPLC-UV-MS/TOF run. (a) UV diode array chromatogram, and extracted ion chromatograms for (b). *m*/*z* 477.1 and (c) *m*/*z* 609.2. Numbers indicate three of the five identified phenylpropanoid glycosides (**1**–**3**) and many of the putative compounds (**6** and **8**–**13**). UV peaks elute slightly earlier than MS peaks. See Table 2 for UV retention times.

many of the PPGs and corresponds to a hydroxytyrosol moiety after water loss, also observed by Cardinali et al. (2012) from verbascoside and various verbascoside derivatives. Other diagnostic ions from disaccharide PPGs consisted of fragments remaining after the loss of only the secondary sugar. These included *m*/*z* 477 or 491 for compounds with caffeoyl or feruloyl moieties, respectively, and unmodified hydroxytyrosol groups, and *m*/*z* 505 for PPGs with both a feruloyl group and a hydroxytyrosol with a single methoxy (compounds **15** and **16**).

2.4. Putative PPGs in M. guttatus

We identified 11 additional putative PPGs from the crude extract used for isolation of compounds **1**–**3** and **5**, and from foliage of individual analyzed plant samples, based upon UV and mass spectral similarities to the five confirmed structures (Table 2, Appendix 1). Nine of these compounds appear to be isomers of **1**, **2** and **3**. First, compounds **6**–**8** all have the same exact mass as **1** and **2** ($[M-H]^-$ *m*/*z* 477) and very similar MS/MS spectrometry fragment patterns, indicating that they are probably also monosaccharide PPGs. Other possible PPGs with the same molecular weight as **1** and **2** include plantainosides A and B (Damtoft and Jensen, 1994; Miyase et al., 1991), calceolarioside D (Nicoletti et al., 1988a), and sanangoside (Jensen, 1994). All four of these contain a caffeoyl moiety that would result in the MS^2 ion fragments of *m*/*z* 161, 179, and 315 observed for compounds **6**–**8**. Plantainoside A and B represent positional isomers of **1** and **2**, with caffeoyl groups attached to the C-3′ or C-2′ carbon of the central glucose, respectively. Calceolarioside D and sanangoside are both somewhat unusual PPGs. Calceolarioside D has a l-hydroxy-4-oxo-2,5-cyclohexadiene group connected to the glucosyl moiety C-1″, instead of the usual hydroxytyrosol, and sanangoside has an allose as the central sugar, instead of glucose (Jensen, 1994). Despite these structural differences, both of these compounds would fragment similar to calceolarioside A and B. Finally, other plant species that synthesize calceolarioside A and B also produce some of the above PPGs, such as plantainoside A in *Chirira sinensis* (Gesneriaceae; Damtoft and Jensen, 1994) and calceolarioside D in various species of Chilean *Calceolaria* (Di Fabio et al., 1995). Next, compounds **9**–**14** have the same exact mass as conandroside (**3**, $[M-H]^-$ *m*/*z* 609) and share many of its UV and mass spectral characteristics. Most notable is the MS^2 ion of *m*/*z* 447, which in conandroside arises from a loss of caffeic acid, leaving hydroxytyrosol attached to a glucose–xylose disaccharide. Other known disaccharide PPGs with the same mass as conandroside include calceolarioside C (Nicoletti et al., 1988a) and E (Nicoletti et al., 1988b). Calceolarioside C is a positional isomer of conandroside with xylose at C-6′. Calceolarioside E has the same overall structure as conandroside, but with apiose instead of xylose as its secondary sugar. Additionally, while all PPGs identified in this study had hydroxycinnamic acids in the (*E*)-configuration, the compounds above can also occur as (*Z*)-isomers, observed for PPGs (Nishimura et al., 1991) and other phenylpropanoid-pathway natural products (Keefover-Ring et al., 2014).

Putative PPGs **15** and **16**, which correspond to PPGs 6 and 7, respectively, in Holeski et al. (2013), shared some MS/MS characteristics with the newly identified compound mimuloside (**5**). In particular, the MS^2 spectra of all three contained a fragment of *m*/*z* 193, which in mimuloside resulted from the loss of a feruloyl moiety. However, **15** also fragmented into ions *m*/*z* 443 and 461 and **16** into 457 and 475, and both into 505 (Table 2, Appendix 1). These fragments suggest the presence of methoxy groups on both the hydroxycinnamic acid and the hydroxyphenylethyl moieties and the identity of the accessory sugar as either xylose (compound **15**) or rhamnose (compound **16**). Known compounds with the same masses as putative PPGs **15** and **16,** with similar expected fragmentation patterns, include aeschynanthosides C (Li et al., 2008) and the isomers martynoside and isomartynoside (Miyase et al., 1991), respectively.

3. Conclusion

This work demonstrates that yellow monkeyflower produces a diverse suite of structurally related phenylpropanoid glycosides. Characterization of these compounds, combined with our earlier work on genetic variation in *M. guttatus* (Holeski et al., 2013),

shows the high level of chemical variation in this species, both within and among individuals. This detailed knowledge of yellow monkeyflower's specialized chemistry represents another useful trait in genetic studies and lays the groundwork for continued exploration of this model species' chemical ecology.

4. Experimental

4.1. Plant material

Yellow monkeyflower [*M. guttatus* DC. (Phrymaceae; Beardsley and Olmstead, 2002)] ranges from Mexico to Alaska in western North America and typically grows in riparian areas and other moist habitats. The plant material used for compound isolation derived from seeds collected from 12 natural populations in California, Oregon, or Washington, USA, and British Columbia, Canada. We grew plants from seed in a greenhouse at the University of Wisconsin – Madison [Fafard 3B potting soil, 16 h days with high-pressure sodium supplemental lighting, bottom-watered daily, and fertilized weekly with Blossom Booster (J.R. Peters, Allentown, PA, USA)]. We harvested foliage from mature, often flowering plants. For the crude extract containing compounds **1**–**3** and **5,** we pooled the leaves from several populations high in these PPGs [see Holeski et al. (2013) and Table A1 in Appendix 2]. The foliage used for the isolation of compound **4** came from population 2 in Holeski et al. (2013) (see Table A1 in Appendix 2), noted for high amounts of this particular PPG. After air drying, we ground all above-ground tissues (mostly leaves and stems) with a Wiley mill (size 20 mesh screen), yielding ~150 and ~100 g of powdered material from the two sources, respectively, which was stored at −20 °C until extraction.

4.2. PPG extraction and isolation

For extraction of compounds **1**–**3** and **5**, we weighed 50 g of powdered plant tissue into a 2 l beaker, added 500 ml of reagent grade hexane, mixed thoroughly and allowed to sit for 5 min, then filtered with a Buchner funnel through #4 Whatman paper. Returning the solid material to the beaker each time, we repeated this step three times with 500 ml of hexane, followed by 2× 500 ml of dichloromethane. We then extracted the washed powdered plant tissue with 4× 250 ml of cold (4 °C) reagent grade MeOH, filtered the resulting solution with a 0.45 μm nylon membrane, discarded the solid material, and evaporated the MeOH extract under reduced pressure to a dark brown tarry consistency. To remove any remaining chlorophyll and non-polar compounds we dissolved the crude extract in 400 ml of 50:50 H_2O:acetone and pumped the solution through a VersaFlash purification system (Sigma–Aldrich Corp., St. Louis, MO, USA) fitted with a 40 × 37.5 mm cartridge packed with ~30 g C_{18}-RP silica gel (10% C, 40–63 μm particle size, Acros Organics, Thermo Fisher, Waltham, MA, USA) which had been primed with 200 ml of 50:50 H_2O:acetone. We evaporated the resulting clear amber-colored liquid under reduced pressure, recovering a light brown solid. We repeated the entire procedure above with 63 g of powdered plant tissue from the population with high concentrations of compound **4**.

We initially purified compounds **1**–**3** and **5** with flash chromatography by dissolving 3.1 g of the crude extract in 50 ml of MeOH combined with enough dry silica gel to make a brown extract-silica powder after evaporation. We then loaded the powder onto a 4 × 20 cm silica gel flash chromatography column poured with $CHCl_3$:MeOH (16:1). Column elution began with 1 l of $CHCl_3$:MeOH (16:1) at 1 bar of air pressure, followed by 900 ml $CHCl_3$:MeOH (8:1), and finally ~650 ml $CHCl_3$:MeOH (4:1). We collected ~20 ml fractions, which were checked with TLC (neat) and/or UHPLC–MS (20 μl vacuum dried and resuspended in 20 μl each of MeOH and H_2O with 0.1% formic acid). We combined similar flash chromatography fractions and evaporated them under reduced pressure.

We further purified selected consolidated flash fractions from the crude extract containing compounds **1**–**3** and **5** using preparative HPLC with a VP 250/21 Nucleodur C_{18} HTEC HPLC column (250 × 21 mm, 5 μm; Macherey-Nagel GmbH & Co. KG, Düren, Germany) with multiple isocratic runs using a mobile phase of H_2O:CH_3CN (65:35; both with 0.005% formic acid) at a flow rate of 20 ml min^{-1}. We monitored the separations with UV at 340 nm and manually collected peaks of the various compounds, combining similar fractions from multiple 1 ml injections of flash fractions dissolved in MeOH. After freezing and lyophilizing the PPG-containing mobile phase solutions, we recovered 29 mg of **1**, 24 mg of **2**, 149 mg of **3**, and 27 mg of **5** as off-white amorphous powders. The crude extract containing compound **4** proved pure enough to further purify directly with preparative HPLC using an Altec C_{18} column (250 × 10 mm, 5 μm; Altec Chromatography, Deerfield, IL, USA) and repeated 250 μl injections of the crude extract dissolved in MeOH using the same conditions as above, except for a flow rate of 7 ml min^{-1}. Combined lyophilized mobile phase fractions collections yielded 11 mg of **4** as a light yellow amorphous powder.

4.3. NMR analyses of compounds *1*–*5*

We characterized the structures of compounds **1**–**5** with ^1H and ^{13}C NMR on a 500 MHz Bruker spectrometer equipped with a cryoprobe (compounds **1**, **3** and **4)** and on 750 (compound **2**) and 400 MHz (compound **5**) Bruker instruments using CD_3OD (99.8% D; Sigma–Aldrich, St. Louis, MO, USA) as the solvent. We dissolved ~5–18 mg of each compound in 0.5 ml of solvent and performed one-dimensional ^1H and ^{13}C NMR and two-dimensional hetero-nuclear single-quantum correlation spectroscopy (HSQC), hetero-nuclear multiple-bond correlation spectroscopy (HMBC), and correlation spectroscopy (COSY) experiments, reporting ^1H and ^{13}C chemical shifts (δ) in ppm relative to CHD_2OD (δ_H = 3.30 ppm for ^1H) or CD_3OD (δ_C = 49.0 ppm for ^{13}C), respectively.

4.4. UHPLC-UV-TOF/MS analyses

We analyzed the crude extract containing compounds **1**–**3** and **5**, an authentic verbascoside standard purified from *Plantago lanceolata* (Plantaginaceae; M.D. Bowers, unpublished data), and six individual plant samples representative of various *M. guttatus* populations with UHPLC using UV and electrospray ionization (ESI) time-of-flight (TOF)/MS detectors. For both the crude extract and the verbascoside standard, we dissolved small amounts in a 50:50 mixture of MeOH and H_2O with 0.1% formic acid. The individual plant sample preparations followed that of Holeski et al. (2013), except that the final dried extracts were redissolved in a 50:50 mixture of MeOH and H_2O with 0.1% formic acid. We injected 2 μl of each sample onto a Waters Acquity UHPLC system, equipped with a 100 × 2.1 mm, 1.7 μm C18 UHPLC column (held at 40 °C) and an Acquity photodiode array (PDA) detector coupled to an LCT Premier ESI-TOF/MS in the negative mode (all from Waters, Milford, MA, USA). We separated compounds in each sample with a binary solvent gradient using water as solvent A and CH_3CN as solvent B, both containing 0.1% formic acid, at a flow rate of 500 μl min^{-1}. The gradient program consisted of 1–20% B over the first 4 min, 20–40% B over the next 2 min, 40–95% B over the next 3 min, held at 95% B for 4.5 min (13.5 min total), and then returned to initial conditions for the next injection. Using the PDA, we continually collected UV data from 210 to 400 nm. MS settings included a source temperature of 120 °C, a cone gas flow of 10 l h^{-1}, desolvation temperature of 320 °C, nebulization gas flow at 600 l h^{-1}, and the capillary and cone voltages at 2.5 kV (negative

ionization mode) and 35 V, respectively. We acquired data every 0.1 s, with a 0.01 s interscan delay and ensured accurate mass measurements using leucine enkephalin as a lock mass compound; directly infusing a 400 pg μl^{-1} 50:50 CH_3CN:H_2O solution at 20 $\mu l\ min^{-1}$. All compounds usually appeared as both their deprotonated ($[M-H]^-$) and formate adduct ($[M-H+FA]^-$) forms.

4.5. High-resolution tandem MS analyses

We gathered additional structural information for compounds isolated from the crude extracts and in individual plant samples with high-resolution MS/MS spectrometry. We injected samples similar to those prepared for UHPLC-TOF/MS on a Thermo Accela LC system fitted with a Hypersil C18 GOLD column (50 × 2.1 mm, 1.9 μm) held at 40 °C coupled to a LTQ Orbitrap high-resolution tandem mass spectrometer operated in the negative mode (all from Thermo Fisher Scientific, Bremen, Germany), using the same mobile phase as for the UHPLC-TOF/MS. We collected mass spectra of the negative precursor ions for all compounds in the Orbitrap mass analyzer after collision-induced dissociation (CID) in the LTQ cell at 35 eV (MS^2). For many of the compounds we also fragmented the most abundant product ion from the precursor ion experiments (MS^3), also at 35 eV.

Acknowledgements

Special thanks to Prof. Søren Jensen for helpful comments on various drafts of this work and confirmation of mimuloside as a new PPG. In addition, the comments from several anonymous reviewers greatly strengthened this paper. We also thank Marcus Carlsson for advice on compound isolation, purification, NMR interpretation, and use of equipment. Maria Ahnlund shared her mass spectrometry expertise and conducted much of the MS/MS work. Greg Barrett-Wilt provided help with MS/MS interpretation. This study made use of the National Magnetic Resonance Facility at Madison (NMRFAM), which is supported by NIH grants P41RR02301 (BRTP/NCRR) and P41GM66326 (NIGMS). We also thank Mark Anderson, Rita Hannah, and Jameson Bothe at NMRFAM for assistance with running NMR samples. The *Mimulus* seed library (Duke University) and D. Lowry generously provided some of the seeds used in this study. Funding for this research was provided by National Science Foundation grants DEB-0425908 and DEB-0841609 to RLL.

Appendix A. Supplementary data

Supplementary data associated with this article can be found, in the online version, at http://dx.doi.org/10.1016/j.phytol.2014.08.016.

References

Beardsley, P.M., Olmstead, R.G., 2002. Redefining Phrymaceae: the placement of *Mimulus*, tribe Mimuleae and Phryma. Am. J. Bot. 89, 1093–1102.
Boeckler, G.A., Gershenzon, J., Unsicker, S.B., 2011. Phenolic glycosides of the Salicaceae and their role as anti-herbivore defenses. Phytochemistry 72, 1497–1509.
Bohm, B.A., 1992. Exudate flavonoids of *Mimulus lewisii*. Biochem. Syst. Ecol. 20, 591.
Cardinali, A., Pati, S., Minervini, F., D'Antuono, I., Linsalata, V., Lattanzio, V., 2012. Verbascoside, isoverbascoside, and their derivatives recovered from olive mill wastewater as possible food antioxidants. J. Agric. Food Chem. 60, 1822–1829.
Chen, R.C., Su, J.H., Yang, S.M., Li, J., Wang, T.J., Zhou, H., 2002. Effect of isoverbascoside, a phenylpropanoid glycoside antioxidant, on proliferation and differentiation of human gastric cancer cell. Acta Pharmacol. Sin. 23, 997–1001.
Chen, Y.J., Zhang, H.G., Li, X., 2009. Phenylethanoid glycosides from the bark of *Fraxinus mandschurica*. Chem. Nat. Compd. 45, 330–332.
Chin, Y.W., Yoon, K.D., Ahn, M.J., Kim, J., 2010. Two new phenylpropanoid glycosides from the aerial parts of *Paederia scandens*. Bull. Korean Chem. Soc. 31, 1070–1072.
Cooper, R., Solomon, P.H., Kubo, I., Nakanishi, K., Shoolery, J.N., Occolowitz, J.L., 1980. Myricoside, an african armyworm antifeedant: separation by droplet countercurrent chromatography. J. Am. Chem. Soc. 102, 7953–7955.
Damtoft, S., Jensen, S.R., 1994. Three phenylethanoid glucosides of unusual structure from *Chirita sinensis* (Gesneriaceae). Phytochemistry 37, 441–443.
Di Fabio, A., Bruni, A., Poli, F., Garbarino, J.A., Chamy, M.C., Piovano, M., Nicoletti, M., 1995. The distribution of phenylpropanoid glycosides in Chilean *Calceolaria* spp. Biochem. Syst. Ecol. 23, 179–182.
Eubanks, M.D., Carr, D.E., Murphy, J.F., 2005. Variation in the response of *Mimulus guttatus* (Scrophulariaceae) to herbivore and virus attack. Evol. Ecol. 19, 15–27.
Fenster, C.B., Ritland, K., 1994. Quantitative genetics of mating system divergence in the yellow monkeyflower species complex. Heredity 73, 422–435.
Froelich, S., Gupta, M.P., Siems, K., Jenett-Siems, K., 2008. Phenylethanoid glycosides from *Stachytarpheta cayennensis* (Rich.) Vahl, Verbenaceae, a traditional antimalarial medicinal plant. Braz. J. Pharmacogn. 18, 517–520.
Hall, M.C., Willis, J.H., 2005. Transmission ratio distortion in intraspecific hybrids of *Mimulus guttatus*: implications for genomic divergence. Genetics 170, 375–386.
Hare, J.D., 2002a. Geographic and genetic variation in the leaf surface resin components of *Mimulus aurantiacus* from southern California. Biochem. Syst. Ecol. 30, 281–296.
Hare, J.D., 2002b. Seasonal variation in the leaf resin components of *Mimulus aurantiacus*. Biochem. Syst. Ecol. 30, 709–720.
Holeski, L.M., 2007. Within and between generation phenotypic plasticity in trichome density of *Mimulus guttatus*. J. Evol. Biol. 20, 2092–2100.
Holeski, L.M., Chase-Alone, R., Kelly, J.K., 2010. The genetics of phenotypic plasticity in plant defense: trichome production in *Mimulus guttatus*. Am. Nat. 175, 391–400.
Holeski, L.M., Keefover-Ring, K., Bowers, M.D., HarnEnz, Z.T., Lindroth, R.L., 2013. Patterns of phytochemical variation in *Mimulus guttatus* (yellow monkeyflower). J. Chem. Ecol. 39, 525–536.
Iossifova, T., Vogler, B., Klaiber, I., Kostova, I., Kraus, W., 1999. Caffeic acid esters of phenylethanoid glycosides from *Fraxinus ornus* bark. Phytochemistry 50, 297–301.
Jensen, S.R., 1994. A reexamination of *Sanango racemosum*. 3. Chemotaxonomy. Taxon 43, 619–623.
Jensen, S.R., 1996. Caffeoyl phenylethanoid glycosides in *Sanango racemosum* and in the Gesneriaceae. Phytochemistry 43, 777–783.
Jimenez, C., Riguera, R., 1994. Phenylethanoid glycosides in plants: structure and biological activity. Nat. Prod. Rep. 11, 591–606.
Keefover-Ring, K., Carlsson, M., Albrectsen, B.R., 2014. 2′-(*Z*)-Cinnamoylsalicortin: a novel salicinoid isolated from *Populus tremula*. Phytochem. Lett. 7, 212–216.
Li, S.M., Yang, X.W., Shen, Y.H., Feng, L., Wang, Y.H., Zeng, H.W., Liu, X.H., Tian, J.M., Shi, Y.N., Long, C.L., Zhang, W.D., 2008. Chemical constituents of *Aeschynanthus bracteatus* and their weak anti-inflammatory activities. Phytochemistry 69, 2200–2204.
Li, L., Tsao, R., Liu, Z.Q., Liu, S.Y., Yang, R., Young, J.C., Zhu, H.H., Deng, Z.Y., Xie, M.Y., Fu, Z.H., 2005. Isolation and purification of acteoside and isoacteoside from *Plantago psyllium* L. by high-speed counter-current chromatography. J. Chromatogr. A 1063, 161–169.
Lincoln, D.E., Walla, M.D., 1986. Flavonoids from *Diplacus aurantiacus* leaf resin. Biochem. Syst. Ecol. 14, 195–198.
Miyase, T., Ishino, M., Akahori, C., Ueno, A., Ohkawa, Y., Tanizawa, H., 1991. Phenylethanoid glycosides from *Plantago asiatica*. Phytochemistry 30, 2015–2018.
Mojica, J.P., Lee, Y.W., Willis, J.H., Kelly, J.K., 2012. Spatially and temporally varying selection on intrapopulation quantitative trait loci for a life history trade-off in *Mimulus guttatus*. Mol. Ecol. 21, 3718–3728.
Mølgaard, P., 1986. Population genetics and geographical distribution of caffeic acid esters in leaves of *Plantago major* in Denmark. J. Ecol. 74, 1127–1137.
Mølgaard, P., Ravn, H., 1988. Evolutionary aspects of caffeoyl ester distribution in dicotyledons. Phytochemistry 27, 2411–2421.
Nicoletti, M., Galeffi, C., Messana, I., Garbarino, J.A., Gambaro, V., Nyandat, E., Marinibettolo, G.B., 1986. New phenylpropanoid glucosides from *Calceolaria hypericina*. Gazz. Chim. Ital. 116, 431–433.
Nicoletti, M., Galeffi, C., Messana, I., Marinibettolo, G.B., Garbarino, J.A., Gambaro, V., 1988a. Phenylpropanoid glucosides from *Calceolaria hypericina*. Phytochemistry 27, 639–641.
Nicoletti, M., Galeffi, C., Multari, G., Garbarino, J.A., Gambaro, V., 1988b. Studies on genus *Calceolaria*. 3. Polar constituents of *Calceolaria ascendens*. Planta Med. 347–348.
Nishimura, H., Sasaki, H., Inagaki, N., Chin, M., Mitsuhashi, H., 1991. Nine phenethyl alcohol glycosides from *Stachys sieboldii*. Phytochemistry 30, 965–969.
Nitsche, H., Egger, K., Dabbagh, A.G., 1969. Deepoxineoxanthin das hauptcarotinoid in blüten von *Mimulus guttatus*. Tetrahedron Lett. 10, 2999–3002.
Nonaka, G., Nishioka, I., 1977. Bitter phenylpropanoid glycosides from *Conandron ramoidioides*. Phytochemistry 16, 1265–1267.
Owen, R.W., Haubner, R., Mier, W., Giacosa, A., Hull, W.E., Spiegelhalder, B., Bartsch, H., 2003. Isolation, structure elucidation and antioxidant potential of the major phenolic and flavonoid compounds in brined olive drupes. Food Chem. Toxicol. 41, 703–717.
Pati, S., Losito, I., Palmisano, F., Zambonin, P.G., 2006. Characterization of caffeic acid enzymatic oxidation by-products by liquid chromatography coupled to electrospray ionization tandem mass spectrometry. J. Chromatogr. A 1102, 184–192.
Piovano, M., Garbarino, J., Tomassini, L., Nicoletti, M., 2009. Cyclohexanones from *Mimulus glabratus* and *M. luteus*. Nat. Prod. Commun. 4, 1637–1638.

Ravn, H., Andary, C., Kovács, G., Mølgaard, P., 1989. Caffeic acid esters as *in vitro* inhibitors of plant pathogenic bacteria and fungi. Biochem. Syst. Ecol. 17, 175–184.

Ryan, D., Robards, K., Prenzler, P., Jardine, D., Herlt, T., Antolovich, M., 1999. Liquid chromatography with electrospray ionisation mass spectrometric detection of phenolic compounds from *Olea europaea*. J. Chromatogr. A 855, 529–537.

Salem, M.M., Capers, J., Rito, S., Werbovetz, K.A., 2011. Antiparasitic activity of *C*-geranyl flavonoids from *Mimulus bigelovii*. Phytother. Res. 25, 1246–1249.

Schmidt, A., Wachtler, B., Temp, U., Krekling, T., Seguin, A., Gershenzon, J., 2010. A bifunctional geranyl and geranylgeranyl diphosphate synthase is involved in terpene oleoresin formation in *Picea abies*. Plant Physiol. 152, 639–655.

Scoville, A.G., Barnett, L.L., Bodbyl-Roels, S., Kelly, J.K., Hileman, L.C., 2011. Differential regulation of a MYB transcription factor is correlated with transgenerational epigenetic inheritance of trichome density in *Mimulus guttatus*. New Phytol. 191, 251–263.

Shimomura, H., Sashida, Y., Adachi, T., 1987. Phenolic glucosides from *Prunus grayana*. Phytochemistry 26, 249–251.

Shroff, R., Vergara, F., Muck, A., Svatos, A., Gershenzon, J., 2008. Nonuniform distribution of glucosinolates in *Arabidopsis thaliana* leaves has important consequences for plant defense. Proc. Natl. Acad. Sci. U.S.A. 105, 6196–6201.

Sticher, O., Salama, O., Chaudhuri, R.K., Winkler, T., 1982. Structural analysis of eukovoside, a new phenylpropanoid glycoside from *Euphrasia rostkoviana* Hayne. Helv. Chim. Acta 65, 1538–1542.

Wu, C.A., Lowry, D.B., Cooley, A.M., Wright, K.M., Lee, Y.W., Willis, J.H., 2008. *Mimulus* is an emerging model system for the integration of ecological and genomic studies. Heredity 100, 220–230.